Two-dimensional (2D) covalent organic framework as efficient cathode for binder-free lithium-ion battery

Yao, Chang-Jiang; Wu, Zhenzhen; Xie, Jian; Yu, Fei; Guo, Wei; Xu, Zhichuan Jason; Li, Dong-Sheng; Zhang, Shanqing; Zhang, Qichun

2020

Yao, C.-J., Wu, Z., Xie, J., Yu, F., Guo, W., Xu, Z. J., ... Zhang, Q. (2020). Two-dimensional (2D) covalent organic framework as efficient cathode for binder-free lithium-ion battery. ChemSusChem, 13(9), 2457-2463. doi:10.1002/cssc.201903007

https://hdl.handle.net/10356/144035

https://doi.org/10.1002/cssc.201903007

DOI: 10.1002/cssc.200((will be filled in by the editorial staff))

Two-Dimensional (2D) Covalent Organic Framework as Efficient Cathodes for Binder-free Lithium-Ion Battery

Chang-Jiang Yao,[a,b]† Zhenzhen Wu, [b,c]† Jian Xie,[b] Fei Yu,[b] Wei Guo,[d] Zhichuan J. Xu,[b] Dong-Sheng Li,[e] Shanqing Zhang,[c]* Qichun Zhang[b]*

Abstract: Searching new organic cathode materials to address their poor cycle stability and low capacity in lithium ion batteries (LIBs) is very important and highly desirable. In this research, a novel two-dimensional (2D) boroxine-linked chemically-active pyrene-4,5,9,10-tetraone (PTO) covalent organic framework (2D PPTODB COFs) has been synthesized as an organic cathode material with remarkable electrochemical properties, including high electrochemical activity (4 redox electrons), safe oxidation potential window (between 2.3V and 3.08V, Li/Li$^+$), superb structural/chemical stability, and strong adhesiveness. A binder-free cathode was obtained by the mixing of a 70 wt% PPTODB and 30 wt% **carbon nanotubes (CNTs) as a conductive additive. Stemmed from the fast kinetics of electrons/ions, high electrochemical activity, and effective π-π interaction between PPTODB and CNTs, the LIBs with the as-prepared cathode exhibits excellent electrochemical performance such as high specific capacity of 198 mAh g^{-1}, superb rate ability (76 %, 1000 mA g^{-1} vs. 100 mA g^{-1}), and a stable coulombic efficiency (CE, ~99.6% at 150th cycle). This work suggests that the concept of binder-free 2D electroactive material could be a promising strategy to approach energy storage with high energy density.**

Introduction

With the ever-increasing energy demands for consumable electric devices and electronic vehicles, reliable and environmental-friendly energy sources become a substantial cornerstone for modern energy storage and conversion technology.[1-9] As one of sustainable energy-storage technologies, organic rechargeable battery, where functional organic chemicals are applied as electrodes, provides a promising solution to meet the demands of green energy with high power/energy density.[10] Different from traditional inorganic compounds generally causing various environmental issues, the novel organic electrode materials are green and renewable.[11] Because the main component of organic materials are light and cheap elements (e.g. carbon, nitrogen, and oxygen), organic-based batteries can be fabricated with flexible structures, high energy density, and potential cost efficiency.[11-12] In addition, the chemical diversity and tunability of organic materials make it much easy and controllable to design a suitable electrode candidate.[13-14] Currently, comparing with other metal-ion batteries, high-performance lithium ion batteries (LIBs) have attracted huge attention due to their obvious advantage of higher energy density.[15-16] Therefore, more and more research efforts have been put into search new organic electrode materials and enhance their performance in lithium ions storage.

In comparison with anode materials, cathode materials have a decisive factor to determinate the practical specific capacity and working voltages of LIBs. Benefitting from the superiority of molecular-level engineering, which enables to adjust the platform voltage, charge/electron conductivity, and integral flexibility, organic cathodes are regarded as a class of forceful candidates for next-generation electrode materials.[14-15] Among the most explored organic structures (carbonyl compounds, organosulfurs, organic salts, and conjugated polymers), carbonyl compounds stand out because of the huge specific capacities of 3350 mAh g^{-1} offered by elemental oxygen.[16] The early research on carbonyl compound (dichloroisocyanuric acid) as the cathode in a primary lithium battery was studied by Williams et al in the 1960's,[17] and a few works about carbonyl compound-based electrodes were reported in 1970 and 1980's.[18] Until recently, conjugated carbonyl compounds such as ketones, quinones, and anhydrides, have been widely re-considered as promising organic electrode materials due to their intrinsic properties such as reversible redox

[a] Dr. C.-J. Yao
State Key Laboratory of Explosion Science and Technology, School of Mechatronical Engineering, Beijing Institute of Technology, Beijing 100081, P. R. China
[b] Dr. C.-J. Yao, Z. Wu, Dr. J. Xie Dr. F. Yu, Prof. Z. Xu, Prof. Q. Zhang
School of Materials Science and Engineering, Nanyang Technological University (Singapore), 639798, Singapore
E-mail: qczhang@ntu.edu.sg
[c] Z. Wu, Prof. S. Zhang
Centre for Clean Environment and Energy, School of Environment and Science, Gold Coast Campus, Griffith University, QLD 4222, Australia.
E-mail: s.zhang@griffith.edu.au
[d] Prof. W. Guo
College of Chemistry, Zhengzhou University, Zhengzhou 450001, P. R. China
[e] Prof. D.-S. Li
College of Materials and Chemical Engineering, Key Laboratory of Inorganic Nonmetallic Crystalline and Energy Conversion Materials, China Three Gorges University, Yichang, Hubei 443002, P.R. China.
C.-J. Yao and Z. Wu contribute equally
Supporting information for this article is given via a link at the end of

stability, adjustable structure, multi-electron reaction and fast kinetics process.[19-22] Since the theoretical specific capacity of pyrene-4,5,9,10-tetraone (PTO) can reach as high as 409 mAh g^{-1}, the PTO-based conjugated carbonyl compounds have been demonstrated as cathodes in lithium batteries with high energy density.[23-26] However, the bottleneck to commercialize organic carbonyl electrodes is the poor cyclability (which is mainly attributed to the side reaction of the dissolved organic material with the electrolyte), poor electronic conductivity due to the limited conjugation, and low volumetric energy density.[27] To address the poor cycling performance issue of carbonyl compounds, polymerization is an efficient way to restrain the dissolution in electrolyte and achieve fast kinetic properties. Coupling reactions between carbon/carbon,[28] carbon/sulfur,[29] or carbon/nitrogen[30] are the popular strategy to elongate the conjugation and decrease the solubility of organic electrode materials in electrolytes. Such reactions would also allow the as-obtained polymer to exhibit longer cycling lifetime than the corresponding monomer.

Comparing to normal polymers, covalent organic frameworks (COFs), where organic molecules are constructed with periodic building blocks to form an extended rigid network through covalent bonds, are competitive for storing and liberating lithium/sodium ions because of their more redox-active centers, higher stability, orderly open channels, and lower solubility.[31] Thus, COFs are attracting more attention due to their ability to facilitate the ions/electrons diffusion path through the nanoporous channels and additional π-π interaction between few layers.[32-34] To date, COFs have been verified as a promising redox-active substrate with multi-electrons transferring reaction. One unique COF accompanying with the conjugated polymeric structure (C=N and benzene) is reported to exhibit 14-electrons redox chemistry and a high reversible capacity of 1536 mAh g^{-1} after 500 cycles.[35] The as-prepared few-layer 2D COFs is fabricated in the presence of CNTs at the preparation process and designed to have π-π interactions with CNTs. Similarly, triazine-based amorphous COFs are reported to the presence of 11/16 redox electrons generating at organic groups (C=N, –NH-) and rings (triazine/piperazine/benzene rings).[33] The strategies of *in-situ* grown with CNTs and mechanical stripping are also applied to obtain thin-layered 2D COFs/CNTs compositions, which advance the lithium ions storage by boosting surface dynamics. Comparable to high-performance anodes, these materials deliver a high reversible capacity of ~ 1000 mAh g^{-1} after 250 cycles at the current density of 0.1 A g^{-1} and voltage of 0.001-3 V (Li/Li$^+$).

Motivated by the superior-performance of COFs anode, COFs based cathode are also deeply explored to show remarkable lithium storage capacity at a higher charge/discharge voltage platform.[36-38] Recently, one 2D nitrogen-rich conjugated polymer framework (CCP), containing redox-active hexaazatrinaphthalene species and cyanovinylene units, is demonstrated to composite with CNTs to form organic cathode for lithium-ions battery.[36] As a result, a specific capacity of ~116 mAh g^{-1}, high capacity retention rate of ~91% after 1000 cycles and high-rate density were obtained. Huang et al. prepared a composite containing few-layer polyimide (PI)-COFs and *in-situ* attached rGO through mechanical milling method, which displayed a higher/faster energy storage ability.[32] After deducting the capacity contribution from rGO, the PI-ECOF-1/rGO50 with 50 wt % rGO delivers a high specific capacity of ~142 mA h g^{-1} at 0.1C during 1.5-3.5 V (Li/Li$^+$, 1C=142 mA h g^{-1}). In other words, only the 50 wt % loading of rGO noticeably could realize 100% utilization of PI-ECOF-1 because of the enhanced ionic/electronic conductivity. However, redox-innocent conductive additives (e.g. CNTs, rGO) will inevitably increase the integral weight and lead to the reduced energy density of whole electrode. Therefore, further research toward COFs-based electrode materials should focus on the enhancement of the capacity contribution from redox-active COFs and the superior energy density of whole batteries.

In this work, a novel 2D covalent organic framework (**Fig. 1**, named as **PPTODB**), consisting of redox-active pyrene-4,5,9,10-tetraone (PTO) species and planar boroxine (B_3O_3) units, is prepared as a binder-free electrode material for Li-ion batteries. Specifically, **PPTODB** has the merits of porous structure, robust B-O linkage, high chemical/thermal stability, and easy processability. The combined superiorities between two functional groups (PTO and B_3O_3) are favourable to obtain excellent mechanic properties, high energy density and long cycling life due to the following reasons: Firstly, PTO moieties not only are marked with high theoretical capacity (~409 mAh g^{-1}), but also possess low Young's modulus (4.2 ± 0.2 GPa). Four redox-active carbonyl groups are concentrated on one small conjugated unit and support the reversible 4 electrons reactions. The Young's modulus of PTO, which is two magnitude smaller than many metal oxide-based cathodes (100-200 GPa),[39] can effectively reduce the mechanical stress during cell cycling and prevent the loose of interparticle mechanical contact with the electrolyte. The soft mechanical properties of PTO compounds will be advantageous to the fabrication of flexible or stretchable battery electrodes.[40-41] Secondly, the rigid skeleton connecting via B_3O_3 moiety can make it easy to stabilize the porous structure and allow the quick diffusion of lithium ions. It is worthy to note that there has been few reports about boron-containing polymers for applications in LIBs because the easy nucleophile attack of boron could result in the decomposition. Since Yaghi group initiated the synthesis of porous COFs based on the molecular dehydration of boronic acids to construct a planar six-membered boroxine (B_3O_3), the boronic acid was widely used as a common motif to form different COF structure.[42] Furthermore, better than the previous binder-free electrode prepared by complex vacuum filtration,[43-44] **PPTODB** exhibits the intrinsic high stickiness for the proposed π-π stacking effects among the exposed B-OH, planar benzene, and carbon nanotubes(CNTs).[45-47] Our electrode is composed by a high content of **PPTODB** (as high as 70 wt %) and conductive additives (30 wt% of CNTs) without the presence of binder. Therefore, beginning with molecular construction and electrode modification, 2D COF **PPTODB** as a binder-free organic cathode is fabricated to realize higher energy/power density, long cycling stability and simple/low cost operation process. The highly efficient binder-free battery shows a high specific capacity of ~ 198 mAh g^{-1}, superb rate ability (76 %, 1000 mA g^{-1} vs. 100 mA g^{-1}), stable coulombic efficiency (CE, ~99.6% at 150th cycle).

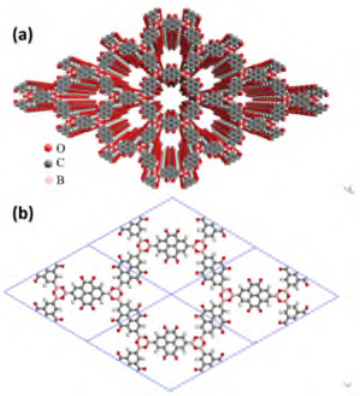

Fig. 1 (a) Illustration of π-π-stacking of 2D **PPTODB**-COFs with redox-active PTO (grey and red) and (b) one-dimensional (1D) channels.

Results and Discussion

Synthesis and characterization of PPTODB

The synthetic route of PPTODB was described in **Fig. 2**.[48] Firstly, compound 2 was prepared via Suzuki borylation of the previously reported compound **1**.[49-51] Then, **2** was hydrolysed with TFA/H_2O, resulting in the intermediate compound PTODB, which was self-assembled into target 2D PPTODB COFs during the simple dehydration of PTODB.[42] The detailed synthesis procedure and characterization data are provided in the supporting information section (**Fig. S1-S6**). However, we cannot obtain well-defined PXRD peaks in the small angle area, and noise peaks in the broad area (20-30°) were always observed. We believed that the material contained crystalized and amorphous forms. All characterization data confirm the successful formation of the as-prepared 2D polymers. The solid state ^{11}B NMR (**Fig. S6**) shows that the center of boron peaks is at 18.47 ppm, which might imply some B-OH existed at the surface or edges for the enhanced interactions between CNTs and 2D PPTODBs.

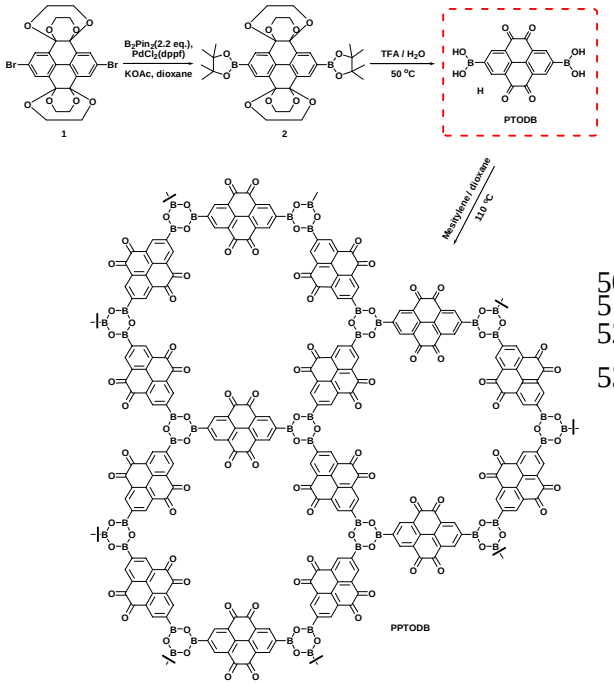

Fig. 2 The construction and synthetic route of **PPTODB**.

In order to further confirm the structure and the stability of **PPTODB**, several characterization technologies such as FT-IR, XPS and TGA have been conducted. From the transmission FT-IR spectrum of **PPTODB** (**Fig. 3a**), electrochemical-active PTO moieties are clearly observed because of the presence of strong C=O vibrational peaks (locating at 1680, 1540 cm^{-1}). Furthermore, the characteristic vibrational bonds of boronate ester ring (B_3O_3) are also found at 1380, 1357, and 1256 cm^{-1}.[52] The peaks at 3435 and 3350 cm^{-1} can be assigned to the vibration of hydroxyl groups, which match well with the results of elemental analysis. X-ray photoelectron spectroscopy (XPS) confirms the composition (C, O and B elements) of **PPTODB** (**Fig. 3b**). Thermogravimetric analysis (**TGA**) indicates that **PPTODB** didn't exhibit obvious decomposition below 275 °C (**Fig. 3c**), suggesting its high thermal stability.

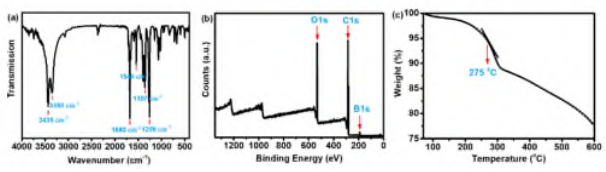

Fig. 3 FT-IR spectra(a), XPS spectra(b) and TGA spectra (c) of **2D PPTODB**.

Field-emission scanning electron microscopy (FESEM) cooperating with energy dispersive X-ray spectrometry (EDS) are performed to observe the morphology and the composition of **PPTODB/MWCNT** binder-free electrode. EDS elemental mapping (**Fig. 4a-c**) confirmed that carbon, oxygen and boron elements uniformly distributed. **Fig. 4 d-f** shows a smooth surface of the electrode with the homogeneous distribution of rod-like **PPTODB** and short CNTs. The big pores, generated by the rods-like **PPTODB**, make it easy for electrolyte diffusion at the electrode.[53] A facile electron transportation path is built because of the evenly attaching of short CNTs at **PPTODB** rods (**Fig. 4 e-f)**.

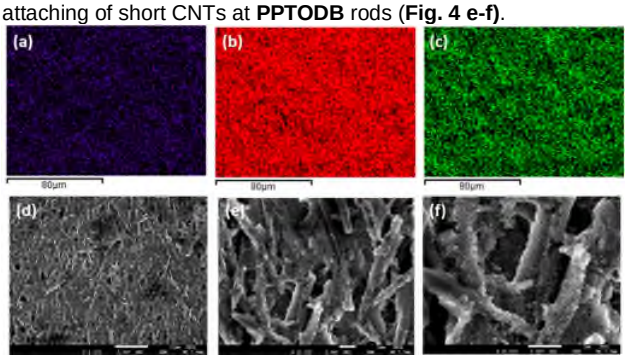

Fig. 4 Elemental mapping (a) Carbon element, (b) Oxygen element, (c) Boron element; (d-f) SEM image of **PPTODB**/MWCNT binder-free electrode film.

Energy storage performance

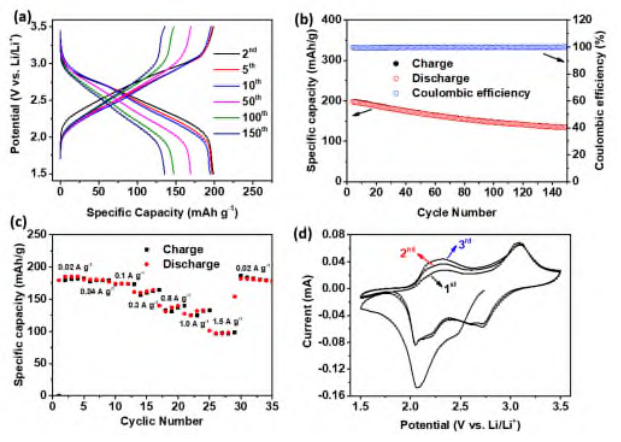

Fig. 5 Electrochemical performance of **PPTODB** between 3.5 and 1.5 V (Li/Li+): a) Charge & Discharge profiles (the 2nd, 5th, 10th, 50th, 100th, & 150th cycles). b) Cycling Performance at 20 mA g^{-1} (for 150 cycles). c) Rate Performance (at different current densities). d) Cyclic Voltammetry curve obtained at the scan rate of 0.1 mV/s.

The charge and discharge data of **PPTODB** at different cycles were obtained at the current density of 20 mA g^{-1} (**Fig. 5a**). **PPTODB** delivered a reversible capacity of 198 mAh g^{-1} at the second discharge process. The stability performance of **PPTODB** has been confirmed by both the high capacity retention of 68.3% and the stable Coulombic efficiency (CE) of ~99.6% (**Fig. 5b**) after the 150th cycling. Rate stability of **PPTODB** was confirmed at different applied current densities as shown in **Fig. 5c**. **PPTODB**

possesses the average capacities of 185, 180, 174, 164, 140, 133 and 98 at the current densities of 20, 40, 100, 300, 800, 1000 and 1500 mA g^{-1}, respectively. When the current density comes back to 20 mA g^{-1}, a recovered capacity of 182 mAh g^{-1} can be gained. All those excellent electrochemical performances demonstrate the great potential of **PPTODB** in rechargeable lithium-ion batteries as an effective organic cathode material.

Proposed redox mechanism

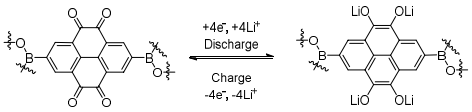

Fig. 6: Electrochemical reaction mechanism of **PPTODB** with lithium ion intercalation/deintercalation during charging/discharging process.

Specifically, the working mechanism of **PPTODB** can be described as the intercalation-deintercalation of the cation species Li^+ during the charging/discharging process (**Fig. 6**). The electrochemically active **PTO** units can theoretically accept and release four lithium ions accompanying with four electrons. According to cyclic voltammogram data (**Fig. 5d**), two obvious separated redox peaks were present at 2.30 and 3.08 V vs. Li^+/Li, showing two redox electrons are transferred at each peak. During the battery process, the **PPTODB** cathode can uptake 2.33 Li^+ upon discharging based on the as-obtained reversible maximum specific capacity of 198 mAh g^{-1} (with a molecular weight of 314 g mol^{-1} per repeating unit), while Li^+ in the $LiPF_6$ salt is plated/stripped from the lithium-metal anode. Therefore, it is concluded that π−π interaction between PPTODB and MWCNTs could strengthen the formation of a flexible film without any binder and further supress the dissolution of the carbonyl-polymers.

Conclusion

In summary, we have prepared a novel 2D **PPTODB** containing highly-active PTO unites via the condensation of intermediate boronic compound monomers. The as-obtained **PPTODB** has been used as a binder-free cathode for lithium ions storage. **PPTODB** as the cathode delivers a maximum capacity of 198 mAh g^{-1} with an average output voltage of 2.8 V, which is mainly contributed from the electrochemically-active PTO moiety. A good reversibility with 68.3% of the initial capacity is retained after 150 cycles. Our results strongly encourage chemists/material scientists to explore other new high-performance 2D COFs through the participation or replacement of PTO for flexible energy storage devices.

Experimental Section

General Information

Unless otherwise noted, the following conditions were applied in our research. All manipulations were performed under an inert atmosphere (dry argon). Bis(pinacolato)diboron (B_2Pin_2) was purchased from Sigma Aldrich Co. Solvents were freshly distilled and deoxygenated. Reaction progress was monitored using thin layer chromatography (TLC) plates pre-coated with a layer of silica with fluorescent indicator UV254. Column chromatography was performed using Silica Gel 60 (40-63 microns) as the stationary phase. Solvents were generally removed in vacuum using a rotary evaporator.

Characterization

^{1}H NMR and **^{13}C NMR** were obtained at room temperature using a Bruker Avance 300 NMR spectrometer with tetramethylsilane (TMS, 0.00 ppm) as an internal standard and $CDCl_3$ as solvent. **Mass spectra** was measured on MALDI Shimadzu Performance (3,5-dimethoxy-4-hydroxycinnamic acid as matrix). **High resolution mass spectra (HRMS)** was recorded on a Water Q-Tof premier mass spectrometer. **Elemental analysis** was conducted on a PerkinElmer 2400Series II CHNS/O elemental analyzer. **Fourier transform infrared (FTIR)** spectroscopy was measured using a PerkinElmer Spectrum Frontier FTIR spectrometer. **Raman spectroscopy** was obtained on the Nicolet iS50 FTIR spectrometer equipped with the iS50 Raman module (excitation wavelength λ = 1064 nm). **Energy dispersive X-ray spectrometry (EDS) elemental mapping** was collected by a Field Emission SEM (FESEM) JEOL/JSM-7600F at an accelerating voltage of 15 kV. **Scanning electron microscopy (SEM)** images were conducted on a JEOL/JSM-6340F at 5 kV. The cells were tested on a NEWRE multichannel battery test system (at room temperature) with the galvanostatic charge and discharge in the range of 3.5-1.5 V for cathode investigations. **Rate performance** was evaluated at different applied current densities of 20 mA g^{-1} → 40 mA g^{-1} → 100 mA g^{-1} → 300 mA g^{-1} → 800 mA g^{-1} → 1000 mA g^{-1} → 1500 mA g^{-1} → 20 mA g^{-1}. The maximum specific capacity 198 mAh g^{-1} at the first cycle was calculated based on the weight of the active cathode material at a current density of 20 mA g^{-1}.

Structural simulation

Although the PPTODB was low crystalline materials as it was obtained as intrinsically exfoliated nanorods, we still tried to simulate the 2D structure by using the Forcite module with a Universal forcefield of material studio (1.Materials Studio v.7.0; Accelrys Software: San Diego, 2013). The possible modelling (AA stacking mode) was considered for the PPTODB. Conventional modelling of PPTODB in fully eclipsed AA stacking mode was carried out using hexagonal (P6/mmm) space group.

Electrode preparation

The as-prepared poly-PTODB polymer sample was mixed with multi-wall CNTs (a weight ratio of 7:3 in NMP solvent). Homogeneous poly-PTODB polymer electrode slurries were prepared via grinding with a pestle for about 50 mins. The slurries were uniformly pasted onto the current collector aluminum foils. The as-prepared smooth electrode films were dried at 60 ℃ in vacuum overnight. The electrode loading is between 1.7-3.1 mg (corresponding to an active poly-PTODB cathode material of around 1.19-2.17 mg).

Battery Fabrication and electrochemical measurements

The electrochemical performance of **PPTODB** cathode was investigated on the 2032 coin-type cells using $LiPF_6$ in EC/DMC (v:v, 1:1) as electrolyte, lithium foil as the counter electrode and the as-prepared film as the cathode, celgard 2400 membrane was used as the separator. The cells were fabricated inside an argon-filled glove box with both the moisture and oxygen levels below 1 ppm. The final assembled cells were placed for an equilibration time of 12 hrs before test initiated, and the first process was the charge process.

The cells were tested on a NEWRE multichannel battery test system (at room temperature) with the galvanostatic charge and discharge in the range of 3.5-1.5 V for cathode investigations. Rate performance was evaluated at different applied current densities of 20, 40, 100, 300, 800, 1000, 1500mA g^{-1} respectively. The maximum specific capacity 205 mAh g^{-1} at the first cycle was calculated based on the weight of the active cathode material at a current density of 20 mA g^{-1}.

Acknowledgements

Q.Z. acknowledges financial support from AcRF Tier 1 (RG 111/17, RG 2/17, RG 114/16, RG 8/16) and Tier 2 (MOE 2017-T2-1-021 and MOE 2018-T2-1-070), Singapore. C.-J. Y. thanks the financial support by the Beijing Institute of Technology. This work was also financially supported by the Australian Research Council (ARC) Discovery Project (DP160102627 and DP1701048343).

Keywords: 2D COFs · Pyrene-4,5,9,10-tetraone · Binder-free cathode · LIBs

[1] X. Zhan, Z. Chen, Q. Zhang, *J. Mater. Chem. A* **2017**, *5*, 14463-14479.

[2] S. Lee, G. Kwon, K. Ku, K. Yoon, S.-K. Jung, H.-D. Lim, K. Kang, *Adv Mater*, **2018**, *30*, 1704682.

[3] T. B. Schon, B. T. McAllister, P.-F. Li, D. S. Seferos, *Chem Soc Rev*, **2016**, *45,* 6345-6404.

[4] Y. Liang, Z. Tao, J. Chen, *Adv. Energy Mater.* **2012**, *2*, 742-769.

[5] A. B. Kaiser, V. Skakalova, *Chem Soc Rev*, **2011**, *40*, 3786-3801.

[6] P. Novák, K. Müller, K. S. V. Santhanam, O. Haas, *Chem. Rev.*, **1997**, *90*, 207-281.

[7] Z. Song, H. Zhou, *Energy Environ. Sci.*, **2013**, *6*, 2280–2301.

[8] S. Muench, A. Wild, C. Friebe, B. Häupler, T. Janoschka, U. S. Schubert, *Chem. Rev.*, **2016**, *116*, 9438−9484.

[9] Y. Morita, S. Nishida, T. Murata, M. Moriguchi, A. Ueda, M. Satoh, K. Arifuku, K. Sato, T. Takui, *Nat Mater*, **2011**, *10*, 947-951.

[10] J. Xie, Q. Zhang, *Small*, **2019**, *15*, 1805061.

[11] J. Xie, P.-Y. Gu, Q. Zhang, *ACS Energy Lett.*, **2017**, *2*, 1985-1996.

[12] J. Xie, Z. Wang, Z. J. Xu, Q. Zhang, *Adv. Energy Mater.* **2018**, *8*, 1703509.

[13] Y. Liang, Z. Chen, Y. Jing, Y. Rong, A. Facchetti, Y. Yao, *J. Am. Chem. Soc.* **2015**, *137*, 4956-4959.

[14] (a) J. Xie, C.-e. Zhao, Z.-Q. Lin, P.-Y. Gu, Q. Zhang, *Chem. Asian J.*, **2016**, *11*, 1489-1511; (b)) Z.-Q. Lin, J. Xie, B. Zhang, J. Li, J.-N. Weng, R.-B. Song, X. Huang, H. Zhang, H. Li, Y. Liu, Z. J. Xu, W. Huang, Q. Zhang, *Nano Energy*, **2017**, *41*, 117-127.

[15] Z. Zhang, M. Liao, H. Lou, Y. Hu, X. Sun, H. Peng, *Adv. Mater*, **2018**, *30*, 19.

[16] T. Yokoji, H. Matsubara, M. Satoh, *J. Mater. Chem. A*, **2014**, *2*, 19347-19354.

[17] D. L. Williams, J. J. Byrne, J. S. Driscoll, *J. Electrochem. Soc.*, **1969**, 2-4.

[18] T. Yamamoto, H. Etori, *Macromolecules* **1995**, *28*, 3371-3379.

[19] K. C. Kim, T. Liu, S. W. Lee, S. S. Jang, *J. Am. Chem. Soc.*, **2016**, *138*, 2374−2382.

[20] Z. Song, Y. Qian, M. L. Gordin, D. Tang,T. Xu, M. Otani, H. Zhan, H. Zhou, D. Wang. *Angew. Chem. Int. Ed.*, **2015**, *54*, 13947-13951.

[21] H. Wang, S. Yuan , D. Ma , X. Huang , F. Meng, X. Zhang, *Adv. Energy Mater.*, **2014**. *4*, 1301651.

[22] Y. Liang, P. Zhang, J. Chen, *Chem. Sci.*, **2013**, *4*, 1330.

[23] T. Nokami, T. Matsuo, Y. Inatomi, N. Hojo, T. Tsukagoshi, H. Yoshizawa, A. Shimizu, H. Kuramoto, K. Komae, H. Tsuyama, J. Yoshida, *J Am Chem Soc*, **2012**, *134*, 19694-700.

[24] A. Jaffe, A. S. Valdes, H. I. Karunadasa, *Chem. Mater.*, **2015**, *27*, 3568-3571.

[25] Q. Li, D. Li, H. Wang, H. Wang, Y. Li, Z. Si, Q. Duan, *ACS Appl. Mater. Interfaces* **2019**, *11*, 28801-28808

[26] M. Yao, H. Senoh, S. Yamazaki, Z. Siroma, T. Sakai, K. Yasuda, *J. Power Sources*, *2010*, *195*, 8336-8340.

[27] J. Wu, X. Rui, G. Long, W. Chen, Q. Yan, Q. Zhang, *Angew. Chem. Int. Ed.*, **2015**, *54*, 7354-7358.

[28] A. Robitaille, A. Perea, D. Bélanger, M. Leclerc, *J. Mater. Chem. A*, **2017**, *5*, 18088; N. Zindy, J. T. Blaskovits, C. Beaumont, J. Michaud-Valcourt, H. Saneifar, P. A. Johnson, D. Bélanger, M. Leclerc, *Chem. Mater.* **2018**, *30*, 6821−6830; Z. Song, Y. Qian, M. L. Gordin, D. Tang, T. Xu, M. Otani, H. Zhan, H. Zhou, D. Wang, *Angew.Chem. Int. Ed.* **2015**, *54*, 13947–13951.

[29] Z. Song , Y. Qian , T. Zhang , M. Otani, H. Zhou, *Adv. Sci.* **2015**, *2*, 1500124.

K. Amin, L. Mao, Z. Wei, *Macromol. Rapid Commun*. **2019**, *40*, 1800565.

[30] H. Kang, H. Liu, C. Li, L. Sun, C. Zhang, H. Gao, J. Yin, B. Yang, Y. You, K.-C. Jiang, H. Long, S. Xin, *ACS Appl. Mater. Interfaces* **2018**, *10*, 37023−37030; C. Su, H. He, L. Xu, K. Zhao, C. Zheng, C. Zhang, *J. Mater. Chem. A*, **2017**, *5*, 2701.

[31] A. P. Côté, A. I. Benin, N. W. Ockwig, M. O' Keeffe, A. J. Matzger, O. M. Yaghi, *Science*, **2005**, *310*, 1166-1170.

[32] Z. Wang, Y. Li, P. Liu, Q. Qi, F. Zhang, G. Lu, X. Zhao, X. Huang, *Nanoscale*, **2019**, *11*, 5330-5335.

[33] Z. Lei, X. Chen, W. Sun, Y. Zhang, Y. Wang, *Adv. Energy Mater.*, **2018**, *9*, 1801010.

[34] S. Wang, Q. Wang, P. Shao, Y. Han, X. Gao, L. Gao, S. Yuan, X. Ma, J. Zhou, X. Feng, B. Wang, *J. Am. Chem. Soc.* **2017**, *139*, 4258-4261.

[35] Z. Lei, Q. Yang, Y. Xu, S. Guo, W. Sun, H. Liu, L.-P. Lv, Y. Zhang, Y. Wang, *Nat. Commun.* **2018**, *9*, 576.

[36] S. Xu, G. Wang, B. P. Biswal, M. Addicoat, S. Paasch, W. Sheng, X. Zhuang, E. Brunner, T. Heine, R. Berger, X. Feng, *Angew. Chem. Int. Ed.* **2019**, *58*, 849-853.

[37] R. Yuan, W. Kang, C. Zhang, *Materials*, **2018**, *11*, 937.

[38] F. Xu, S. Jin, H. Zhong, D. Wu, X. Yang, X. Chen, H. Wei, R. Fu, D. Jiang, *Sci Rep*, **2015**, *5*, 8225.

[39] F. P. McGrogan, T. Swamy, S. R. Bishop, E. Eggleton, L. Porz, X. Chen, Y.-M. Chiang, K. J. Van Vliet, *Adv. Energy Mater.* **2017**, *7*, 1602011.

[40] F. Hao, X. Chi, Y. Liang, Y. Zhang, R. Xu, H. Guo, T. Terlier, H. Dong, K. Zhao, J. Lou, Y. Yao, *Joule*, **2019**, *3*, 1–11.

[41] J. Lopez, D. G. Mackanic, Y. Cui, Z. Bao, *Nat. Rev. Mater.*, **2019**, *4*, 312-330.

[42] A. P. Côté, A. I. Benin, N. W. Ockwig, M. O' Keeffe, A. J. Matzger, O. M. Yaghi, *Science*, **2005**, *310*, 1166-1170.

[43] H. Wu, S. A. Shevlin, Q. Meng, W. Guo, Y. Meng, K. Lu, Z. Wei, Z. Guo, *Adv. Mater.* **2014**, *26*, 3338.

[44] C. Ban, Z. Wu, D. T. Gillaspie, L. Chen, Y. Yan, J. L. Blackburn, A. C. Dillon, *Adv. Mater.* **2010**, *22*, 145.

[45] Z. Yang, Z. Wang, X. Tian, P. Xiu, R. Zhou, *J. Chem. Phys.*, **2012**, *136*, 025103.

[46] Hsun Su, Y., et al., *Appl. Phys. Lett.*, **2011**, *99*, 163102.

[47] P. M. Ajayan, J. M. Tour, *Nature*, **2007**, *447*, 1066-1068.

[48] S. Kawano, M. Baumgarten, D. Chercka, V. Enkelmann, K. Mullen, *Chem Commun*, **2013**, *49*, 5058-5060.

[49] J. Xie, W. Chen, G. Long, W. Gao, Z. J. Xu, M. Liu, Q. Zhang, *J. Mater. Chem. A*, **2018**, *6*, 12985-12991.

[50] Z. Guo, Y. Ma, X. Dong, J. Huang, Y. Wang, Y. Xia, *Angew. Chem. Int. Ed.* **2018**, *57*, 11737-11741.

[51] T. Nokami, T. Matsuo, Y. Inatomi, N. Hojo, T. Tsukagoshi, H. Yoshizawa, A. Shimizu, H. Kuramoto, K. Komae, H. Tsuyama, J. Yoshida, *J. Am. Chem. Soc.* **2012**, *134*, 19694-19700.

[52] S. Wan, J. Guo, J. Kim, H. Ihee, D. Jiang, *Angew. Chem. Int. Ed*, **2008**, *47*, 8826-8830.

[53] Z. Wu, J. Xie, Z. J. Xu, S. Zhang, Q. Zhang, *J. Mater. Chem. A*, **2019**, *7*, 4259-4290.

Received: ((will be filled in by the editorial staff))
Published online: ((will be filled in by the editorial staff))

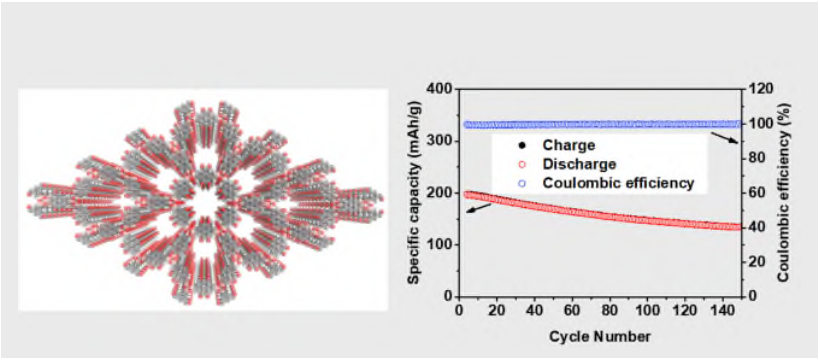

Chang-Jiang Yao,[a,b†] Zhenzhen Wu,[b,c†] Jian Xie,[b] Fei Yu,[b] Wei Guo,[d] Zhichuan J. Xu,[b] Dong-Sheng Li,[e] Shanqing Zhang,[c] Qichun Zhang[b*]*

Page No. – Page No.

Two Dimensional (2D) Covalent Organic Framework as Efficient Cathodes for Binder-free Lithium-Ion Battery

A novel two-dimensional (2D) covalent organic framework (2D **PPTODB** COFs) containing boroxine units and chemically-active pyrene-4,5,9,10-tetraone (PTO) species has been synthesized and demonstrated to show high electrochemical activity (4 redox electrons), safe oxidation potential (2.3V and 3.08V, Li/Li^+), and superb structural/chemical stability. This 2D **PPTODB/CNTs** binder-free cathode exhibits a high specific capacity of 198 mAh g^{-1}, superb rate ability (76 %, 1000 mA g^{-1} vs. 100 mA g^{-1}), and a stable coulombic efficiency (CE, ~99.6% at 150th cycle).